RESEARCH MEMORANDUM

PERFORMANCE OF VARIABLE TWO-DIMENSIONAL INLET DESIGNED FOR ENGINE-INLET MATCHING I - PERFORMANCE AT DESIGN MACH NUMBER OF 3.07

By M. A. Beheim and L. W. Gertsma

Lewis Flight Propulsion Laboratory
Cleveland, Ohio

NATIONAL ADVISORY COMMITTEE
FOR AERONAUTICS

WASHINGTON

November 20, 1956

ERRATA

NACA RESEARCH MEMORANDUM E56H23

By M. A. Beheim and L. W. Gertsma

1956

The following changes should be made:

Page 24, figure 10(a): The key to the symbols should be as follows:

- ○ 15-30 (Design)
- □ 16-31
- ◇ 15-29
- △ 14-29
- ▽ 12-24
- ◿ 19-34
- ◸ 15-31

Issued 3-5-58

NATIONAL ADVISORY COMMITTEE FOR AERONAUTICS

RESEARCH MEMORANDUM

PERFORMANCE OF VARIABLE TWO-DIMENSIONAL INLET DESIGNED FOR ENGINE-INLET MATCHING

I - PERFORMANCE AT DESIGN MACH NUMBER OF 3.07

By M. A. Beheim and L. W. Gertsma

SUMMARY

An investigation of the performance at the design Mach number of 3.07 was conducted on a two-dimensional inlet which had incorporated into its design features necessary for efficient engine-inlet matching over a wide range of flight Mach numbers. The inlet could be operated with either a two-oblique-shock ramp or an isentropic compression surface, both of which could be varied to control the amount of external compression. Provisions for a variety of bypass systems were incorporated and none decreased pressure recovery by more than about 1 percent. Removing about 5 percent of the diffuser airflow through a boundary-layer ram scoop at the diffuser throat increased pressure recovery from 55 to 64 and 70 percent with the two-shock and isentropic ramps, respectively, but decreased subcritical stability by about one-half. Bleeding air near the diffuser exit had little effect on pressure recovery or stability. Diffuser-exit air distortion was about 5 percent at critical operation. Theoretical cowl-pressure drag was equal to about 10 percent of the net thrust of an assumed engine.

INTRODUCTION

The experimental performances of several variable-geometry inlets designed for matching turbojet-engine airflow requirements up to about a Mach number of 2 have been reported in numerous references (e.g., refs. 1 and 2). Theoretical analyses show that if similar matching techniques (i.e., variable external-compression-surface geometry and internal bypass arrangements) are employed with an inlet sized for efficient matching at higher flight Mach numbers (e.g., Mach 3), about 35 percent or more of the air may be spilled at lower flight speeds. Additional experimental data are needed to determine the performance of such inlets.

An investigation was conducted at the NACA Lewis laboratory at several Mach numbers to determine the performance (pressure recovery, mass flow, stability, and distortion) of a two-dimensional inlet, which had incorporated into its design features necessary for efficient engine-inlet matching over a wide range of flight speed. The investigation was not intended to illustrate the matching of any particular engine but was to determine the effects of ramp rotation and bypass arrangements on diffuser performance. This report presents the performance of this diffuser at the design Mach number, 3.07.

SYMBOLS

D_b drag associated with air bleed

F_n net thrust

$F_{n,i}$ ideal net thrust (100-percent pressure recovery)

m mass flow

P total pressure

p static pressure

Subscripts:

b upstream of bottom control door

0 conditions in free stream in capture area of inlet

1 inlet throat

2 compressor face

APPARATUS

The five matching arrangements (which could be used individually or in some combination) considered in the design of the diffuser for operation over a wide range of Mach numbers (see fig. 1) were: (1) supersonic spillage with the compression surface; (2) throat bypass with a ram scoop (which could also be used for boundary-layer removal); (3) top bypass with a flow divider; (4) top bypass without a flow divider; and (5) bottom bypass. Although the throat and top bypasses are shown with the two-shock ramp and the bottom bypass is shown with the isentropic ramp, any of the bypass arrangements could be used with either of the ramps.

In the present investigation at the design Mach number, none of these bypass systems were used as such; however, the effects of removing compression-surface boundary layer through the ram scoop at the throat and also through the bottom bypass were determined. The discharge of the air in both cases was controlled with the bottom control door.

The diffuser was designed to accommodate either a two-oblique-shock ramp or an isentropic compression surface by changing the side fairing. The ramps are shown in figures 1(a) and (b) at the design position (i.e., theoretical compression waves focused at cowl lip) for a Mach number of 3.07. The theoretical pressure recoveries at this Mach number, considering only shock losses, are 72 and 77 percent with the two-shock and the isentropic ramps, respectively.

The angular position of the two-shock ramp could be varied by rotating each of the two ramps about its leading edge. The isentropic ramp also could be rotated about its leading edge, and, since the portion of the ramp with isentropic compressive turning was made of spring steel, the contour could be varied. The subsonic portion of the diffuser could be varied by moving the splitter plate in a vertical direction and by rotating the diffuser plate about its trailing edge. The over-all diffuser length was kept constant, but the length of the diffuser plate was varied for various matching arrangements. The long diffuser plate was used when excess air was to be spilled with either the compression ramp, the throat bypass, or the top bypass. The short diffuser plate was employed when the bottom bypass was to be used.

As indicated in figure 1(a), the initial theoretical external cowl lip angle was 31° (just under shock detachment at the design Mach numb) and the internal angle was 28°. The theoretical pressure drag of this cowl is about 10 percent of the net thrust of a constant rotational speed engine with afterburning at a Mach number of 3. The actual cowl that was used differed slightly from the theoretical cowl in that the lip was bent downward to an external angle of 39° in the region of the cowl leading edge. Because this error did not affect the position of the cowl leading edge with respect to the theoretical position, it probably did not affect internal duct performance appreciably.

The flow-area variations of the diffuser are shown in figures 1(c) and (d). Removing the flow divider of the top bypass resulted in local overdiffusion and discontinuous area variations. Shortening the diffuser plate to use the bottom bypass had similar effects on the area variation.

PROCEDURE

The investigation was conducted in the Lewis 18- by 18-inch Mach number 3.07 tunnel at a Reynolds number of about 1.9×10^6 per foot. Airflow through the diffuser was controlled with a choked exit plug, and the mass-flow ratio was computed from the plug sonic area and a measured average total pressure just upstream of the plug. The pressure recovery was determined in an annulus about a simulated compressor hub with a rake designed for area-weighting (fig. 1(b)). With the throat ram scoop used, the total pressure of the bleed air was measured just upstream of the bottom control door. Critical operation of the inlet was determined from schlieren observation.

During subcritical operation, two distinct types of normal-shock instability were generally observed: (1) a local oscillation of the shock (flutter) accompanied by small fluctuations of compressor face pressure; and (2) a large movement of the shock along the compression surface (buzz) resulting in large variations in compressor-face pressure. As the diffuser mass-flow ratio was decreased, the start of buzz was easily detected because of the large disturbances that resulted. Decreasing airflow further resulted in increased frequency of the disturbances. The start of flutter was not so easily determined, because the frequency and amplitude of the disturbances gradually increased as airflow was decreased. Transient static-pressure fluctuations were measured at the compressor face. Arbitrarily, the normal shock was considered stable until the amplitude (max. to min. values) of the static-pressure fluctuation was greater than 0.4 pounds per square inch ($\Delta p_2/P_0 \approx 0.028$). The stability of the inlet is indicated in this report by the symbols shown in figure 2, which shows examples of the transient compressor-face static-pressure recordings taken during stable operation, flutter, and buzz (arranged in order of decreasing mass-flow ratio). The accuracy of the indicated large amplitudes during buzz is doubtful because of the limitations of the recording equipment.

RESULTS AND DISCUSSION

Optimum Throat Bleed

With the throat ram scoop at a raised position, the operation of the bleed duct could be varied with the bottom control-door position while maintaining critical diffuser operation with the exit-plug position. From the data obtained in this manner (see fig. 3), an optimum control-door position was determined. With the door at this position, the diffuser performance (fig. 4) was obtained by varying the exit-plug position.

Figure 3 presents the critical pressure recovery of the basic diffuser (long diffuser plate and flow divider in place), the bleed mass-flow ratio and total-pressure recovery, and an efficiency parameter for various ram scoop heights and diffuser mass-flow ratios with the ramps at the design positions (theoretical compression waves focused at cowl lip). The scoop was progressively raised until the resulting change in diffuser critical recovery was small. Without boundary-layer removal the critical pressure recovery was much less than the theoretical recovery and was about the same for both the two-shock and the isentropic ramps, although the theoretical recovery of the isentropic ramp was greater. Bleeding air through the scoop resulted in large increases in critical pressure recovery. For example, by removing between 5 and 6 percent of the diffuser airflow, the critical pressure recovery increased from 55 percent with no bleed to 64 and 70 percent with the two-shock and the isentropic ramps, respectively. As shown in figure 3, with the two-shock ramp and a given scoop position the highest diffuser critical recovery occurred when the bleed duct was near choking.

These pressure recoveries compare closely with those obtained with the two-shock and isentropic ramp inlets of reference 3. The supersonic diffusers of the referenced tests differ from the present ones in that they incorporate some internal contraction which reduced the cowl pressure drag to about 2 percent of the engine thrust. It would appear possible to match successfully the low-drag configurations of reference 3 by the method of this report.

These performance characteristics of the primary and bleed airflows were used in evaluating the efficiency parameter shown in figure 3. This parameter is defined as the net thrust of an assumed constant rotational speed engine operating with the measured diffuser pressure-recovery-minus-theoretical-drag incurred from the bleed air divided by the net thrust of the engine operating with 100-percent diffuser pressure recovery. The bleed air was assumed to be discharged downstream in the flight direction from a sonic nozzle. With a given scoop height the efficiency was an optimum at about the same operating condition of the bleed duct for which critical pressure recovery was highest. For the two-shock ramp an optimum scoop-to-throat-height ratio occurred at a lower value than that needed for maximum critical pressure recovery. With the isentropic ramp the optimum scoop-to-throat-height ratio probably was near the highest value for which data are shown.

Inlet Performance Curves

The performance of the diffuser with the two-shock and the isentropic ramps at the design positions is shown in figure 4 for various scoop heights. At each scoop height the control door of the bleed duct was positioned to produce the highest efficiency (determined in fig. 3), and this position was kept fixed as the diffuser airflow was varied with the plug.

Without boundary-layer removal, subcritical stability was fairly extensive with either ramp but was greater with the two-shock ramp. However, stability was decreased by about one-half when the scoop was raised. Air distortion at the compressor face during critical operation without boundary-layer removal was about 5 percent with either ramp (average Mach number just upstream of compressor hub was about 0.3 at critical operation) but increased sharply during supercritical operation and also at slightly subcritical mass-flow ratios with the isentropic ramp. Distortion generally was about 1 percent less when boundary-layer removal was employed, and the sharp rise in distortion at slightly subcritical airflows with the isentropic ramp no longer occurred. In general, varying the control-door position over the range indicated in figure 3 had little effect on distortion at a given scoop height.

Discharge Contours

Some examples of pressure-recovery contours at the compressor face are shown in figure 5. Figures 5(a) and (b) illustrate the changes that occurred at critical operation with the two-shock ramp when boundary layer was removed. Figures 5(c), (d), and (e) show the large variations in distortion that occurred with the isentropic ramp from supercritical to critical to subcritical operation, respectively, without boundary-layer removal. The contour that resulted during critical operation with boundary-layer removal is shown in figure 5(f).

Schlieren Photographs

Without boundary-layer removal the critical mass-flow ratios were somewhat less than 1. Schlieren photographs (fig. 6) indicate that at critical operation a local disturbance (indicated by the arrow) existed just ahead of the cowl lip and may have caused this small loss in airflow. This disturbance may have been a result of interaction between the side fairing boundary layer and the cowl lip shock. The shock from the cowl lip was slightly curved near the cowl leading edge, because the actual external cowl angle, being in error, exceeded the shock detachment angle in this region.

Effects of Roughness and Fillets

Certain of the configurations were rerun with a 1/8-inch-wide strip of number 60 carborundum dust 1/8 inch downstream of the first-ramp leading edge, and the results are shown in figure 7. With boundary-layer removal the effect of roughness with either ramp was small; but without boundary-layer removal and with roughness the pressure recovery with the two-shock ramp (fig. 7(a)) was lower and the distortion was greater, and with either ramp the subcritical stability was less.

A portion of the data also was repeated with 1/2-inch-radius fillets in the corners of the subsonic diffuser. The distortion, in general, was worse with the fillets than without, and other performance characteristics were not improved. Data for these results are not presented.

Flow Survey at Throat

Results of a total-pressure survey of the flow into the inlet at the cowl lip station during critical operation are shown in figure 8 for both ramps at design and off-design positions. When the compression surfaces were at the design position, a vortex sheet was inside the cowl with the two-shock ramp (fig. 8(a)) but outside with the isentropic ramp (fig. 8(c)). Raising the two-shock ramp 1/2° placed the vortex sheet outside the cowl (fig. 8(b)), and changing the isentropic contour slightly, as indicated in figure 9, placed the vortex sheet inside the cowl (fig. 8(d)).

Inlet Performance at Off-Design Geometries

The performance of the inlet with these and other off-design ramp positions is shown in figure 10. The changes in performance probably resulted primarily from the change in the vortex-sheet position indicated in figure 8. Without boundary-layer removal (fig. 10(a)) raising the two-shock ramp above the design position resulted in increased subcritical pressure recoveries and decreased subcritical stability, but lowering the ramp decreased pressure recovery and increased stability. Distortions during critical operation were higher with some ramp positions both above and below the design position. Raising the ramp with boundary-layer removal (fig. 10(b)) produced higher critical pressure recoveries and, in some cases, higher distortions. When the isentropic contour was varied as shown in figure 9 so that the vortex sheet entered the cowl, pressure recovery was appreciably less with corresponding ram-scoop positions, but the sharp rise in distortion which occurred during subcritical operation without boundary-layer removal at the design contour was eliminated.

Influence of Bypass

The flow divider of the top bypass was removed in order to reduce mechanical complexity. The effects of the resulting local overdiffusion and sharp turns on the performance are shown in figure 11. With either compression surface and corresponding scoop positions, pressure recovery was generally about 1 percent less without the flow divider than with it during critical operation. Distortion during critical and subcritical operation with boundary-layer removal was slightly less than when the

divider was in, and the rise in distortion at subcritical operation with the isentropic ramp and no boundary-layer removal was eliminated. In addition, the sharp rise in distortion during supercritical operation was greatly reduced. An example of the change in the pressure-recovery contours of the compressor face that occurred during supercritical operation is shown in figure 12.

With the short diffuser plate in position (bottom bypass arrangement) local overdiffusion again occurred, and the effects on performance are presented in figure 13. For this configuration, bleed air through the throat scoop was not controlled with the bottom control door but was discharged from the chamber beneath the diffuser plate through holes in the chamber walls into the free stream. The maximum mass-flow ratios with the short diffuser plate were somewhat less than with the long plate for corresponding ramp and scoop positions, probably as a result of some model leakage. Pressure recovery was about 1 percent less. Distortion was as much as 3 percent greater with the short diffuser plate than with the long plate and again increased sharply during subcritical operation using the isentropic ramp without boundary-layer removal (fig. 13(b)). Several critical points are also shown on the figure with various amounts of bleed through the bottom bypass. Bleeding up to about one-half of the air in this manner produced slight improvements in distortion but had little effect on pressure recovery and subcritical stability. Removing the flow divider had the same effects as with the long diffuser plate, so data are not presented.

SUMMARY OF RESULTS

An investigation was conducted on the performance of a two-dimensional inlet which had incorporated into its design features necessary for efficient engine-inlet matching over a wide range of flight Mach numbers. The inlet could be operated with either a two-oblique-shock ramp or an isentropic compression surface, which could be varied to regulate the amount of external compression, with a variety of bypass arrangements. The following results were obtained at the design Mach number of 3.07:

1. The critical pressure recovery of the basic diffuser (without bypass arrangements) with either the two-oblique-shock or the isentropic ramps at their design positions and without boundary-layer control was about 55 percent. Diffuser-exit air distortion, which was about 5 percent at critical operation with both ramps, increased rapidly for supercritical operation and also increased sharply with the isentropic ramp at slightly subcritical airflows.

2. By removing the compression-surface boundary layer at the throat of the diffuser with a ram scoop, large improvements were made in pressure recovery. For example, by removing between 5 and 6 percent of the diffuser airflow the critical pressure recovery of the basic diffuser was increased to 64 and 70 percent with the two-oblique-shock and the isentropic ramps, respectively. The sharp increase in distortion for slightly subcritical operation with the isentropic ramp was eliminated. However, subcritical stability was only one-half as large when the ram scoop was raised.

3. The theoretical cowl pressure drag was equal to about 10 percent of the net thrust of an assumed engine.

4. The presence of any of the bypass arrangements generally did not decrease the pressure recovery by more than 1 percent.

5. When the flow divider of the top bypass was removed, resulting locally in overdiffusion, distortion was less during supercritical operation. The bottom bypass also produced local overdiffusion, and distortion at critical operation was as much as 3 percent higher. Bleeding up to about one-half of the air through the bottom bypass (located near the diffuser exit) had little effect on pressure recovery or subcritical stability.

Lewis Flight Propulsion Laboratory
National Advisory Committee for Aeronautics
Cleveland, Ohio, September 12, 1956

REFERENCES

1. Obery, Leonard J., Stitt, Leonard E., and Wise, George A.: Evaluation at Supersonic Speeds of Twin-Duct Side-Intake System with Two-Dimensional Double-Shock Inlets. NACA RM E54C08, 1954.

2. Beheim, Milton A., and Englert, Gerald W.: Effects of a J34 Turbojet Engine on Supersonic Diffuser Performance. NACA RM E55I21, 1956.

3. Woollett, Richard R., and Connors, James F.: Zero-Angle-of-Attack Performance of Two-Dimensional Inlets Near Mach Number 3. NACA RM E55K01, 1956.

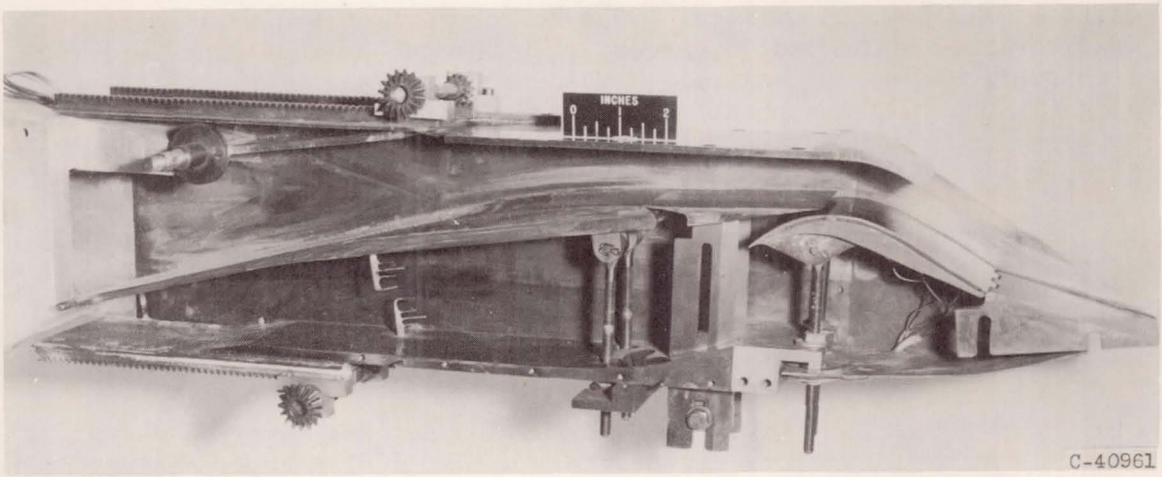

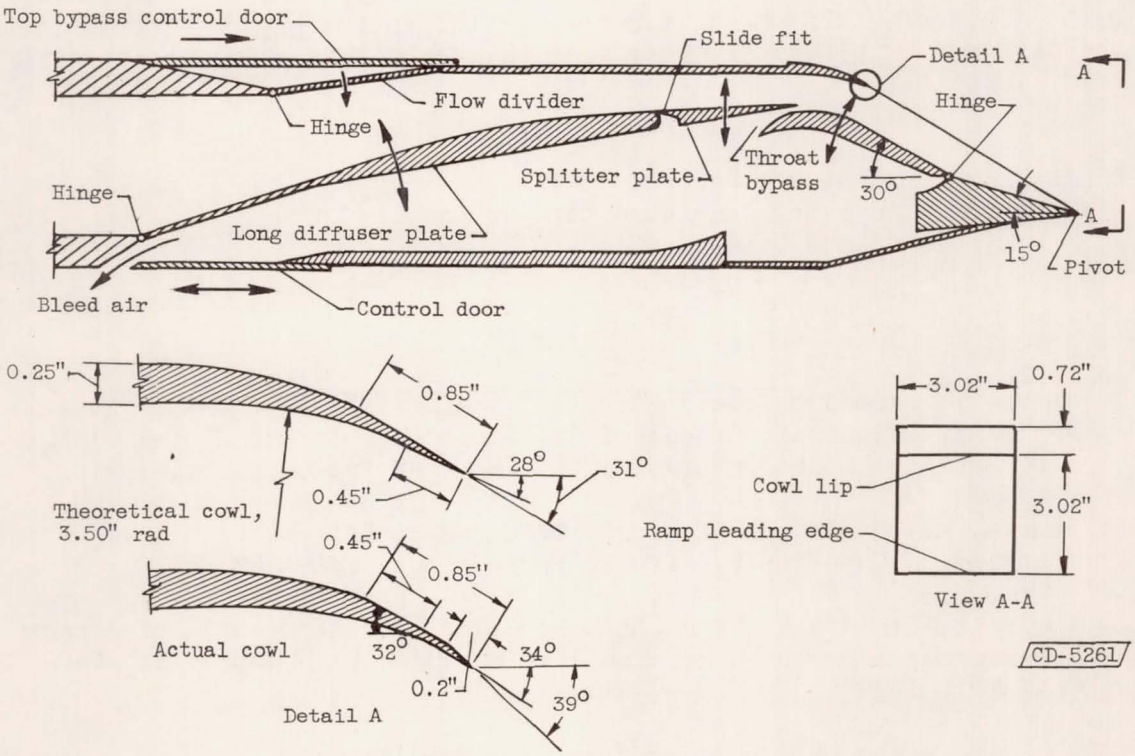

(a) Two-shock ramp and top and throat bypass arrangements.

Figure 1. - Diffuser geometry.

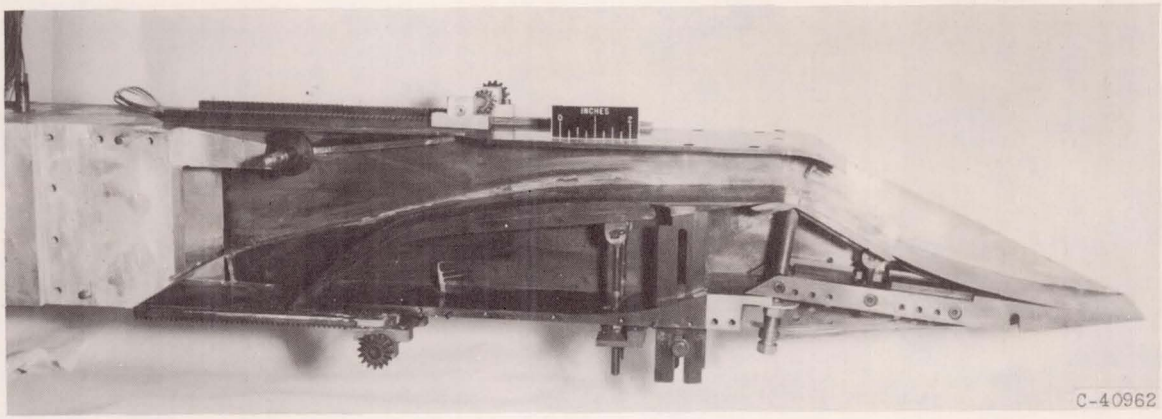

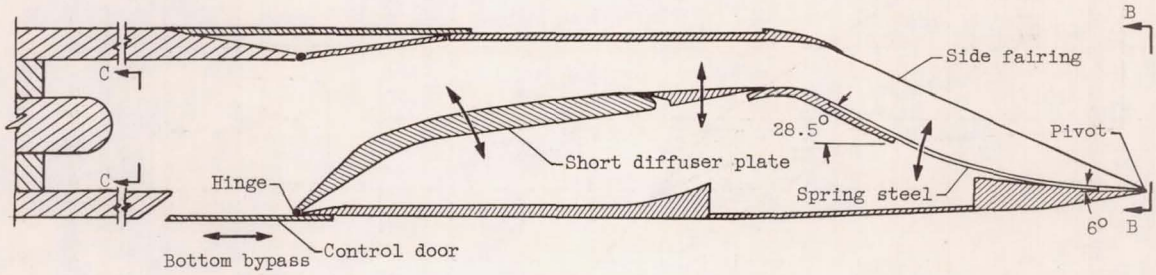

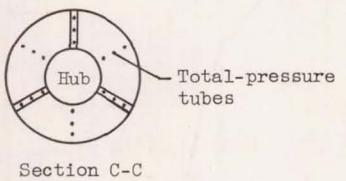

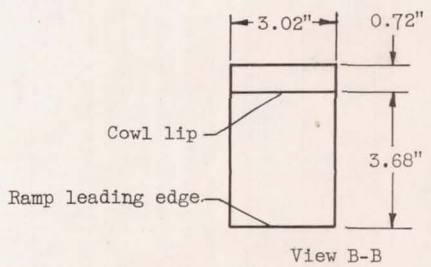

CD-5260

(b) Isentropic ramp and bottom bypass arrangement.

Figure 1. - Continued. Diffuser geometry.

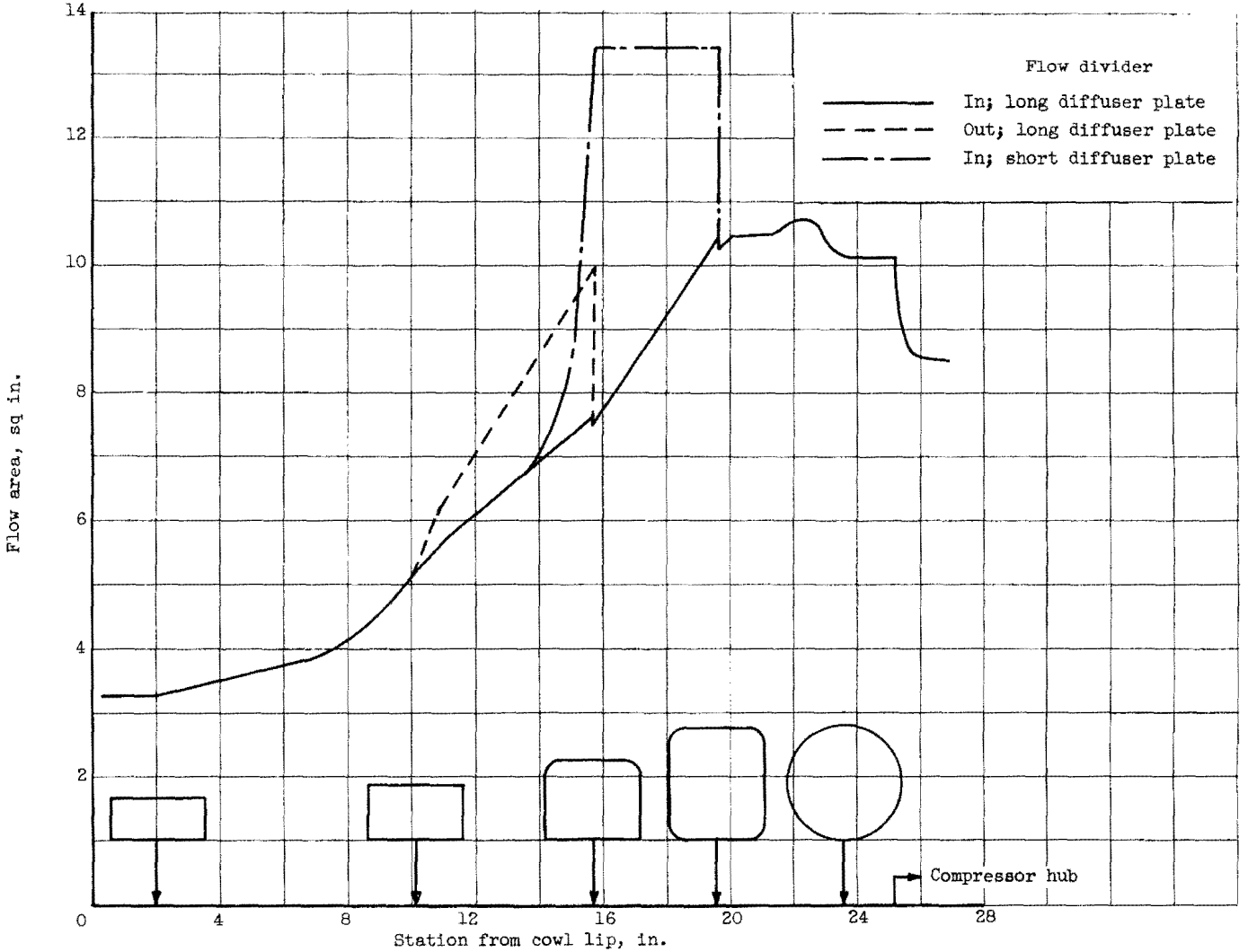

(c) Flow-area variations with two-shock ramp at design position; scoop-to-throat-height ratio, 0.

Figure 1. - Continued. Diffuser geometry.

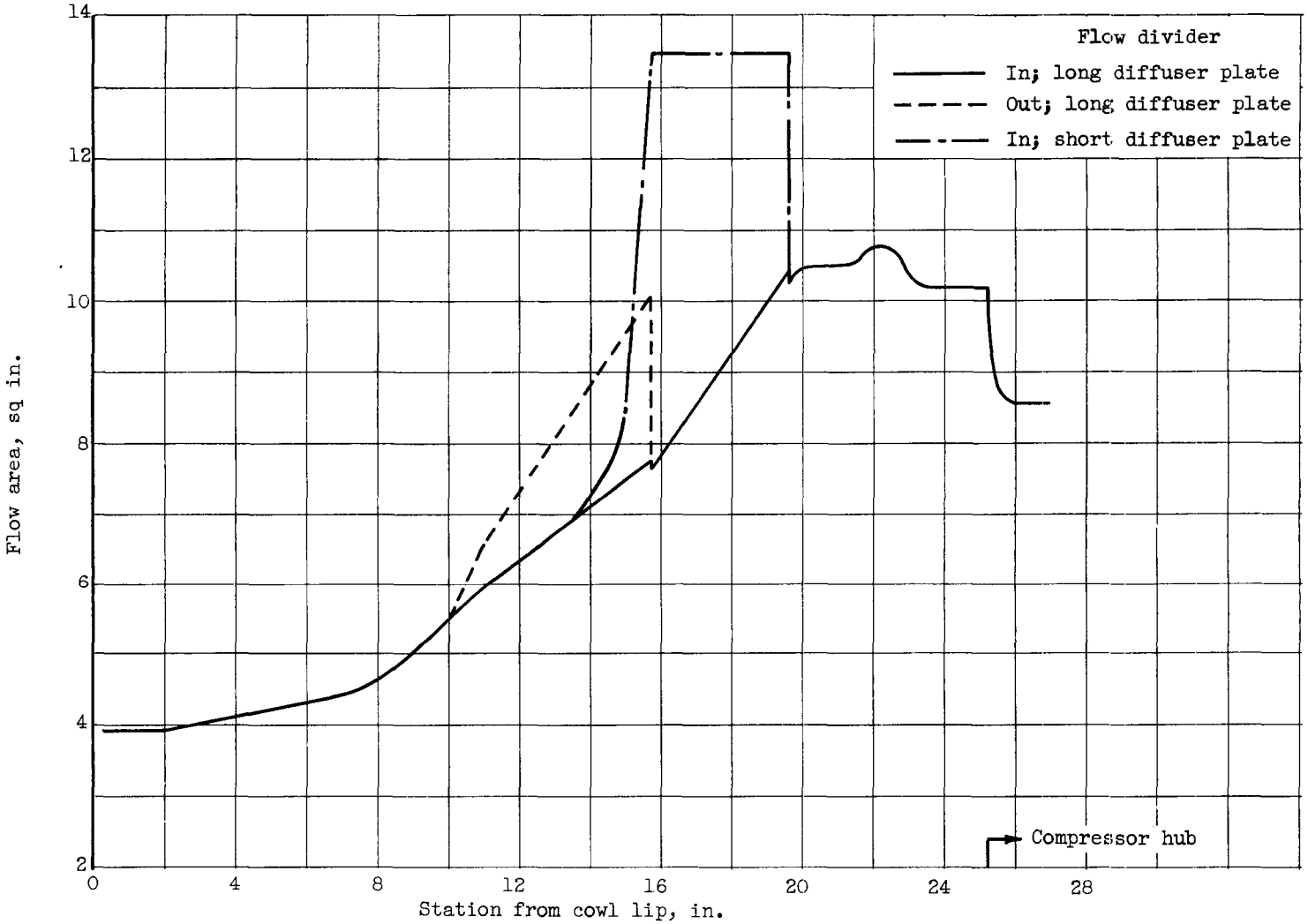

(d) Flow-area variations with isentropic ramp at design position; scoop-to-throat-height ratio, 0.

Figure 1. - Concluded. Diffuser geometry.

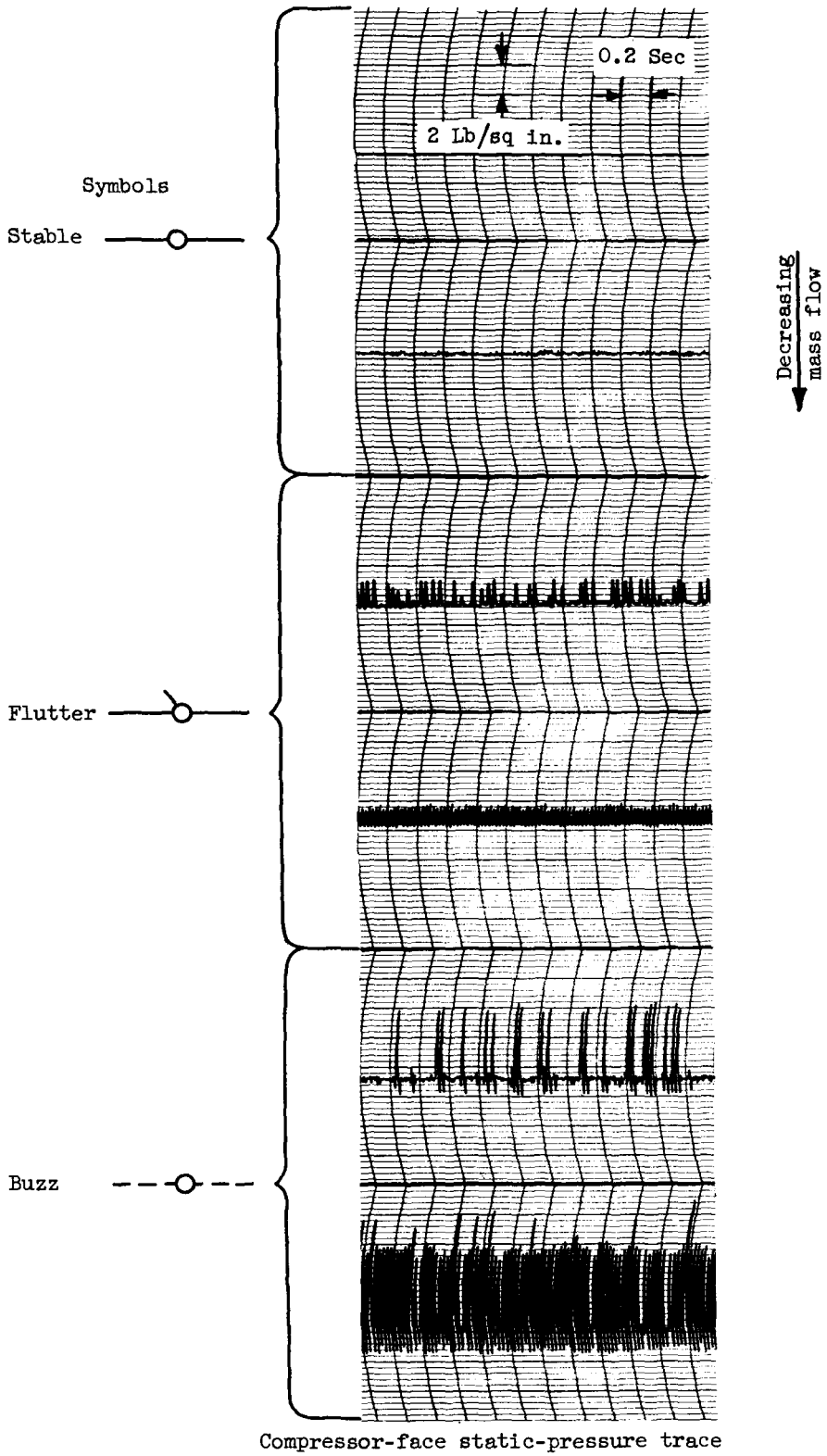

Figure 2. - Definition of inlet stability symbols.

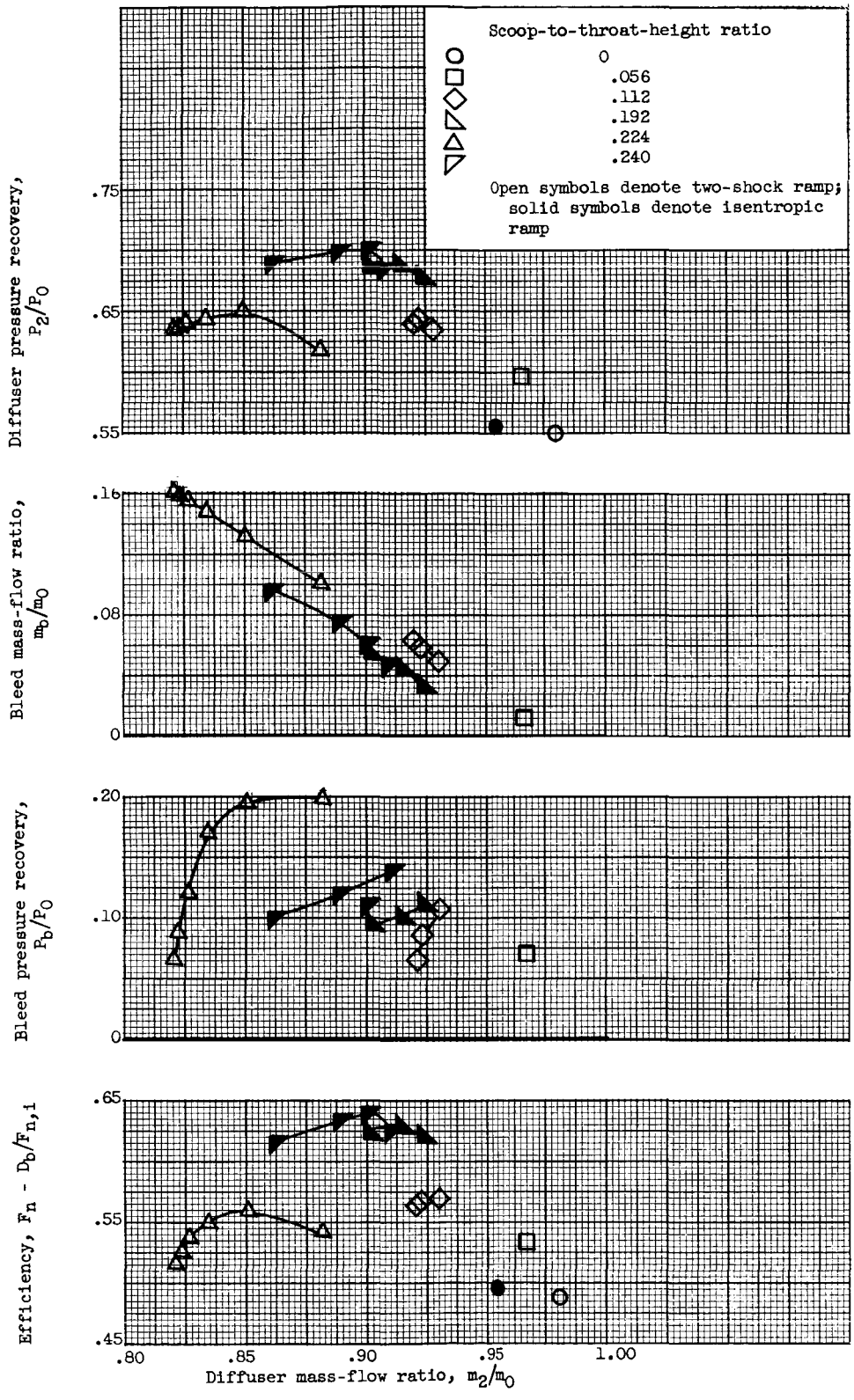

Figure 3. - Effect of throat bleed on basic inlet performance.

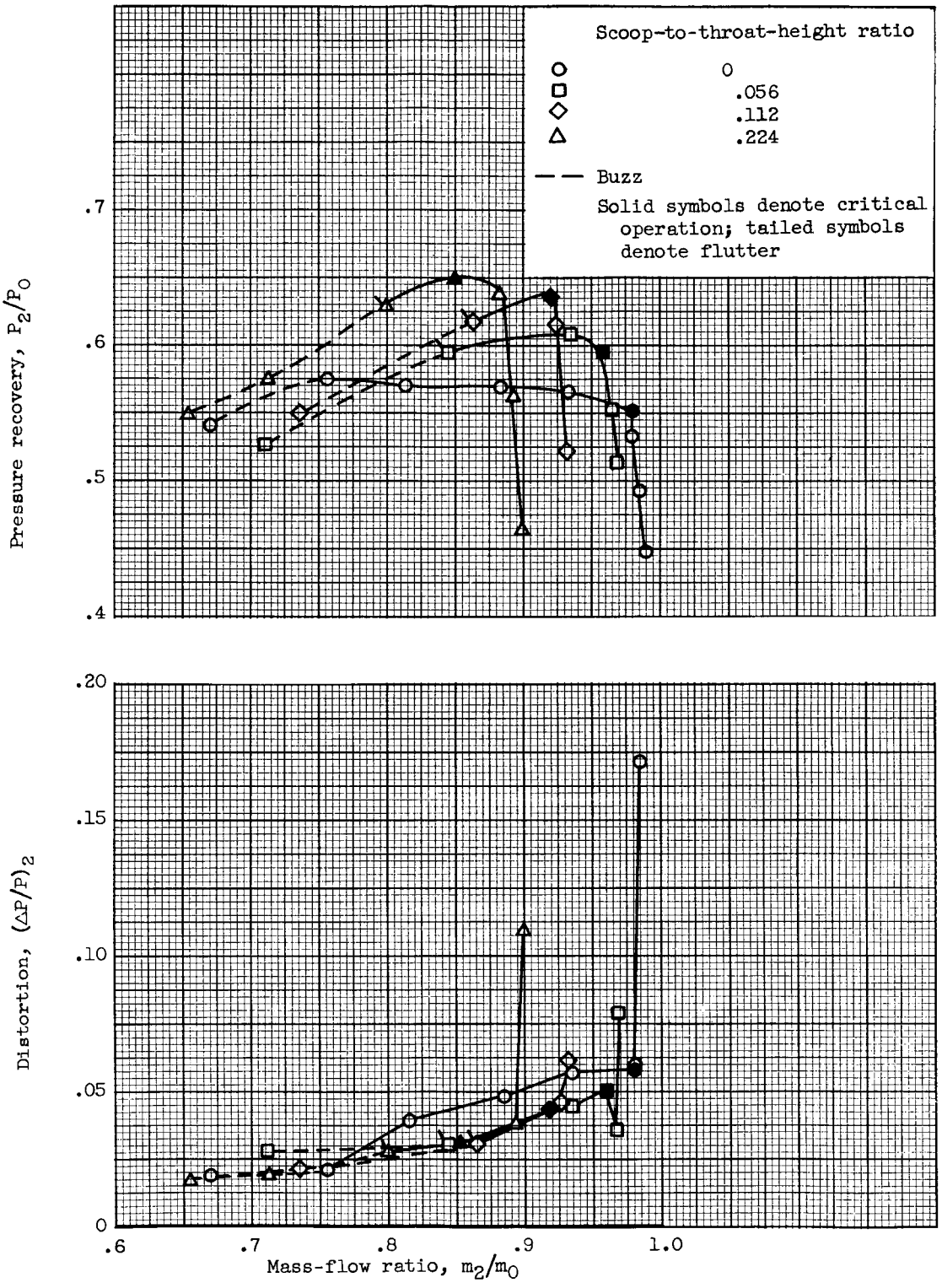

(a) Two-shock ramp.

Figure 4. - Performance of basic diffuser with design ramp positions.

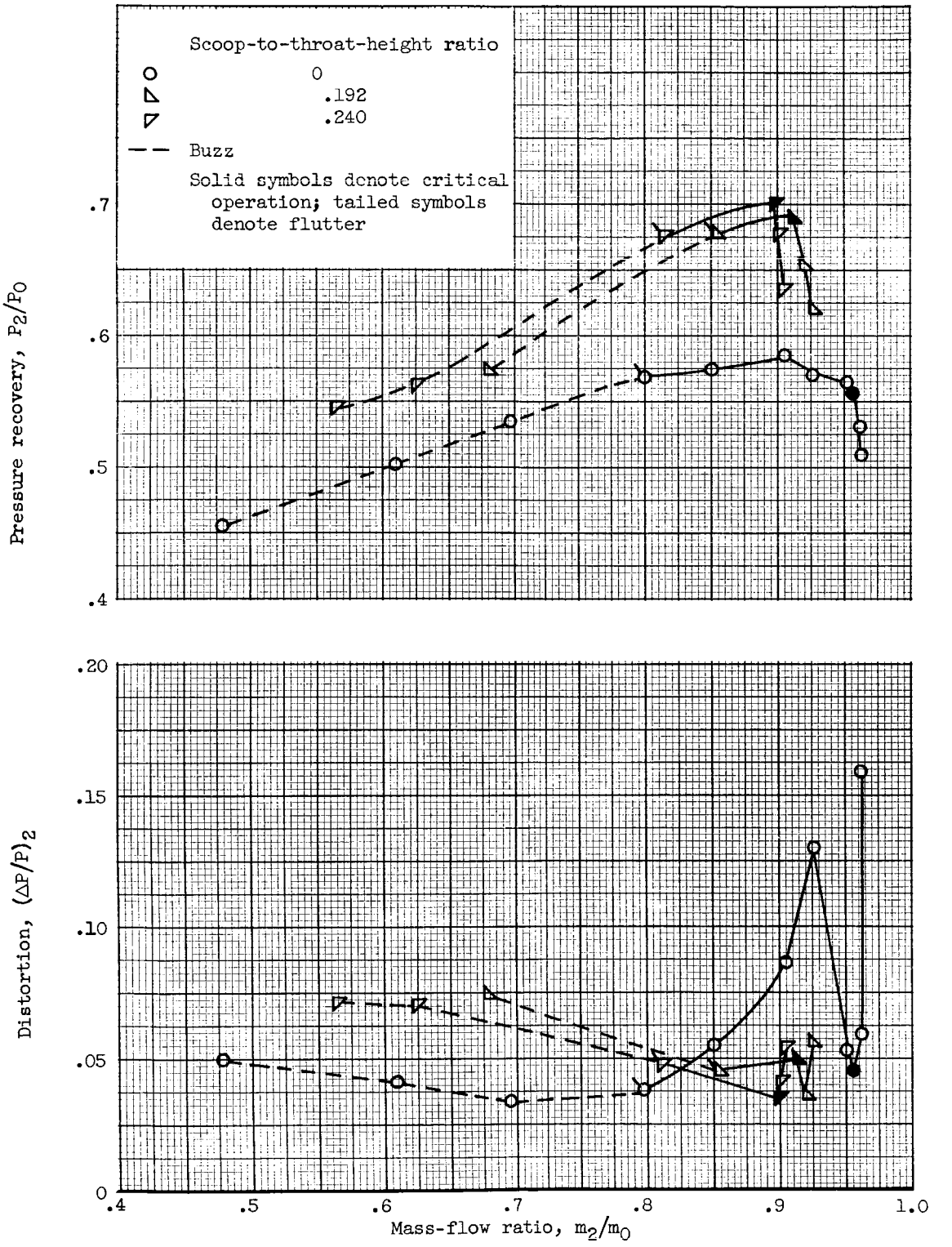

(b) Isentropic ramp.

Figure 4. - Concluded. Performance of basic diffuser with design ramp positions.

Diffuser pressure recovery, P_2/P_0

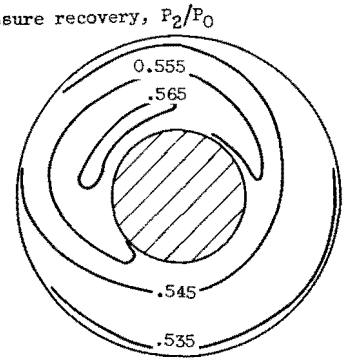

(a) Two-shock ramp; scoop-to-throat-height ratio, 0; critical operation.

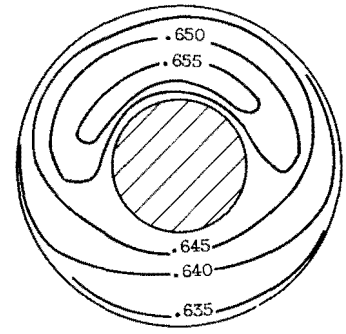

(b) Two-shock ramp; scoop-to-throat-height ratio, 0.224; critical operation; mass-flow ratio, 0.85.

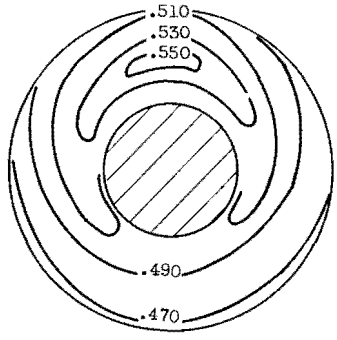

(c) Isentropic ramp; scoop-to-throat-height ratio, 0; supercritical operation; diffuser pressure recovery, 0.51.

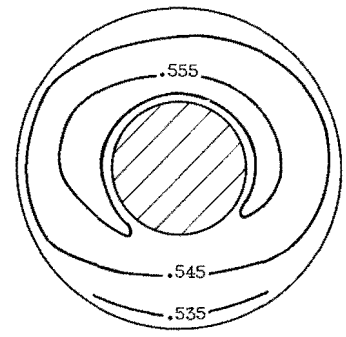

(d) Isentropic ramp; scoop-to-throat-height ratio, 0; critical operation.

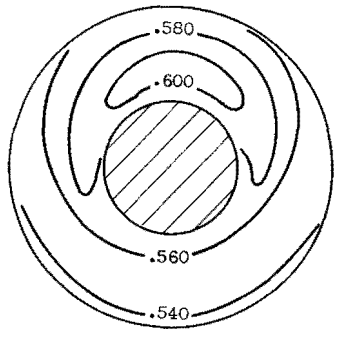

(e) Isentropic ramp; scoop-to-throat-height ratio, 0; subcritical operation; mass-flow ratio, 0.92.

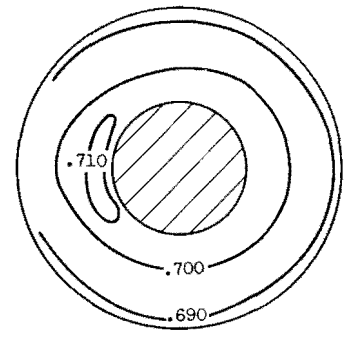

(f) Isentropic ramp; scoop-to-throat-height ratio, 0.240; critical operation; mass-flow ratio, 0.90.

Figure 5. - Pressure-recovery contours at compressor face with basic diffuser and design ramp positions.

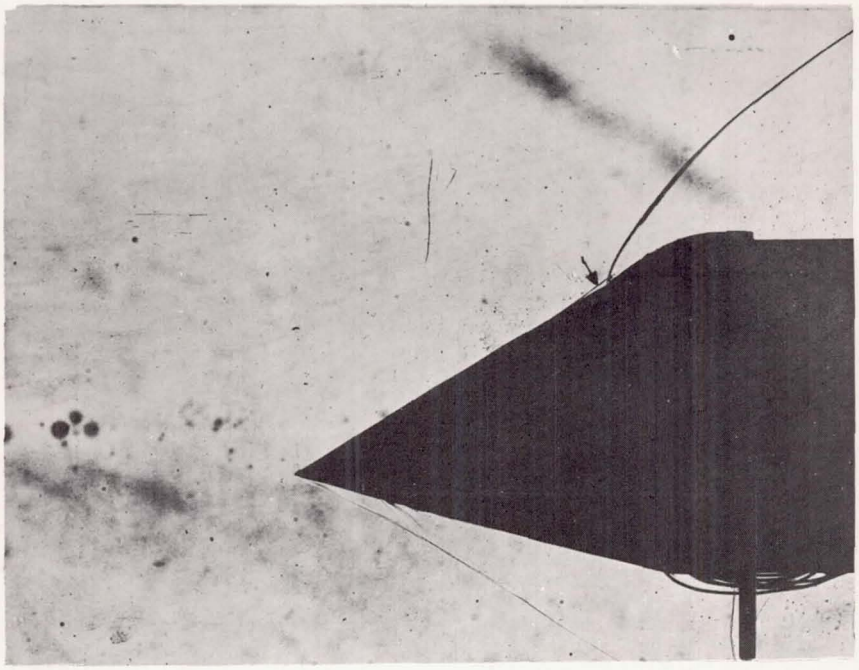

(a) Two-shock ramp.

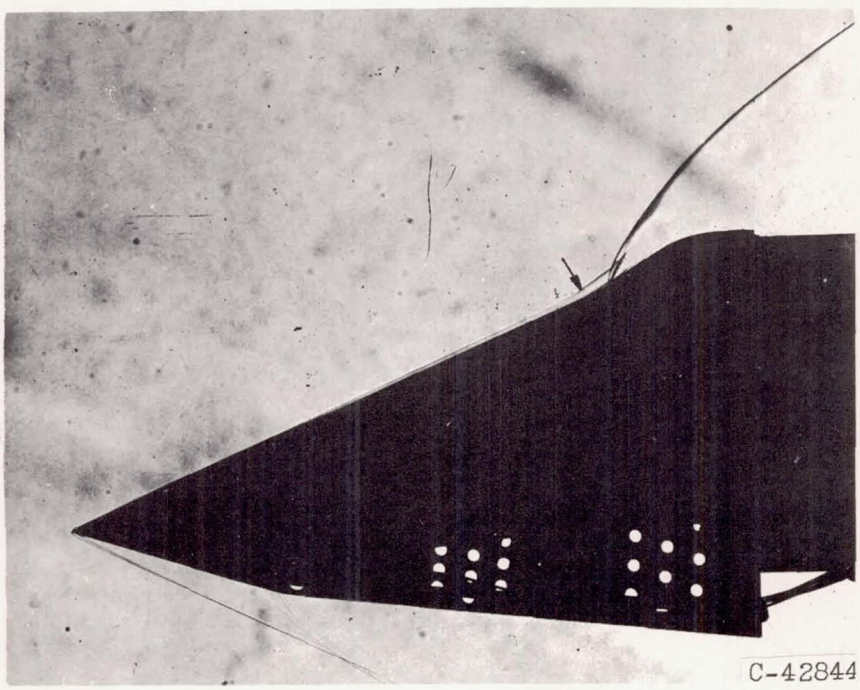

(b) Isentropic ramp.

Figure 6. - Schlieren photographs of model with design ramp positions; critical operation.

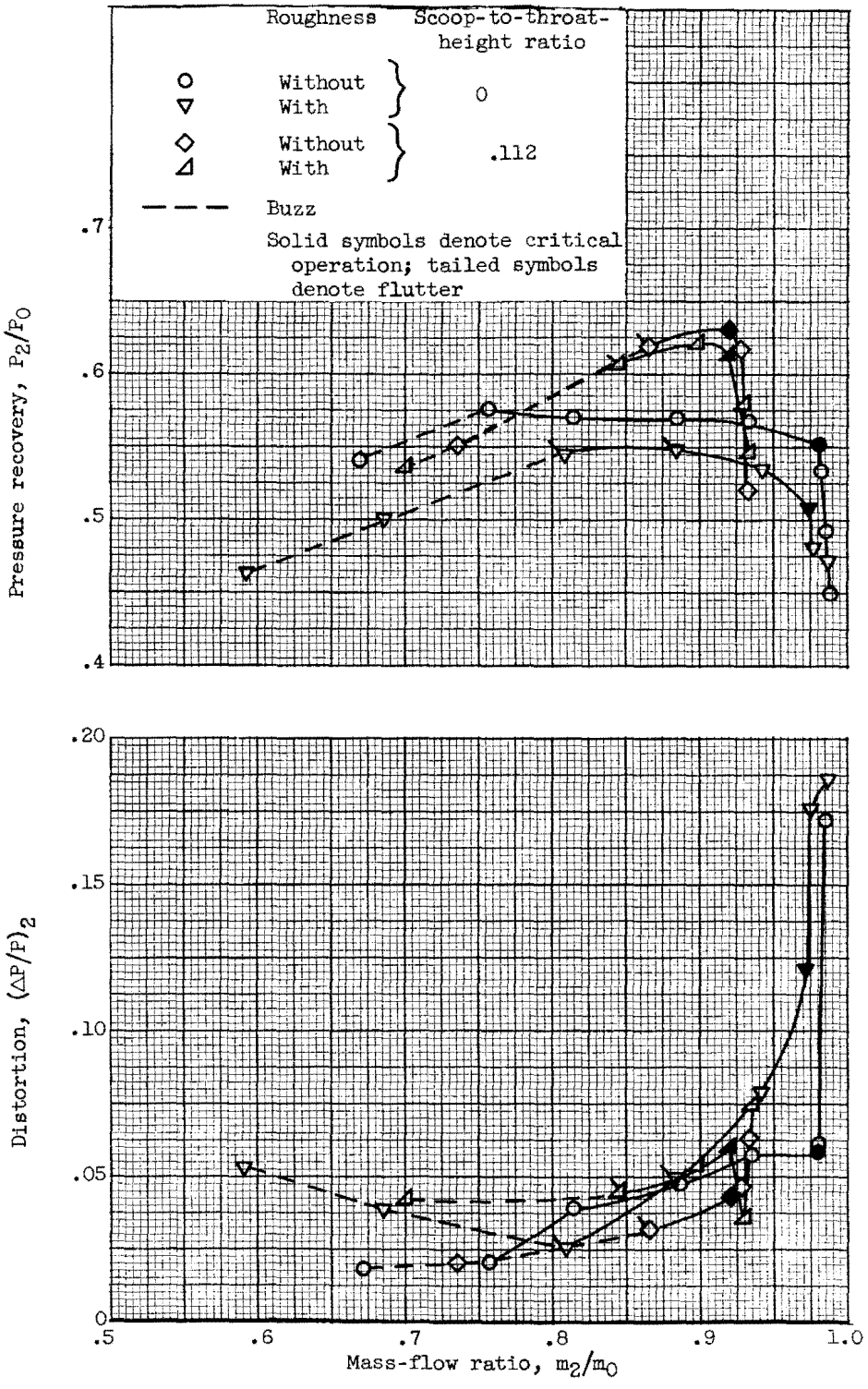

(a) Two-shock ramp.

Figure 7. - Effect of roughness on basic diffuser performance with design ramp positions.

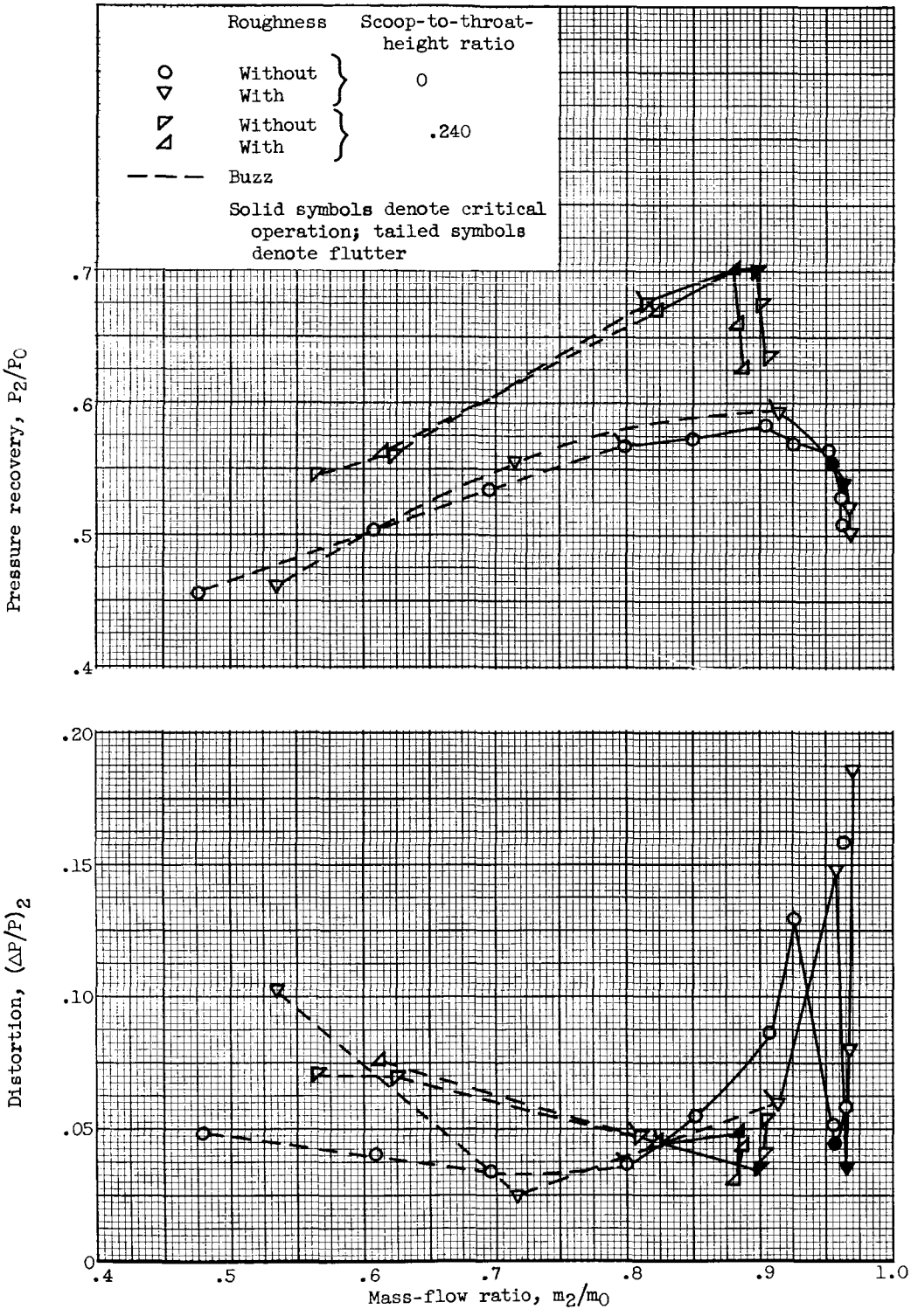

(b) Isentropic ramp.

Figure 7. - Concluded. Effect of roughness on basic diffuser performance with design ramp positions.

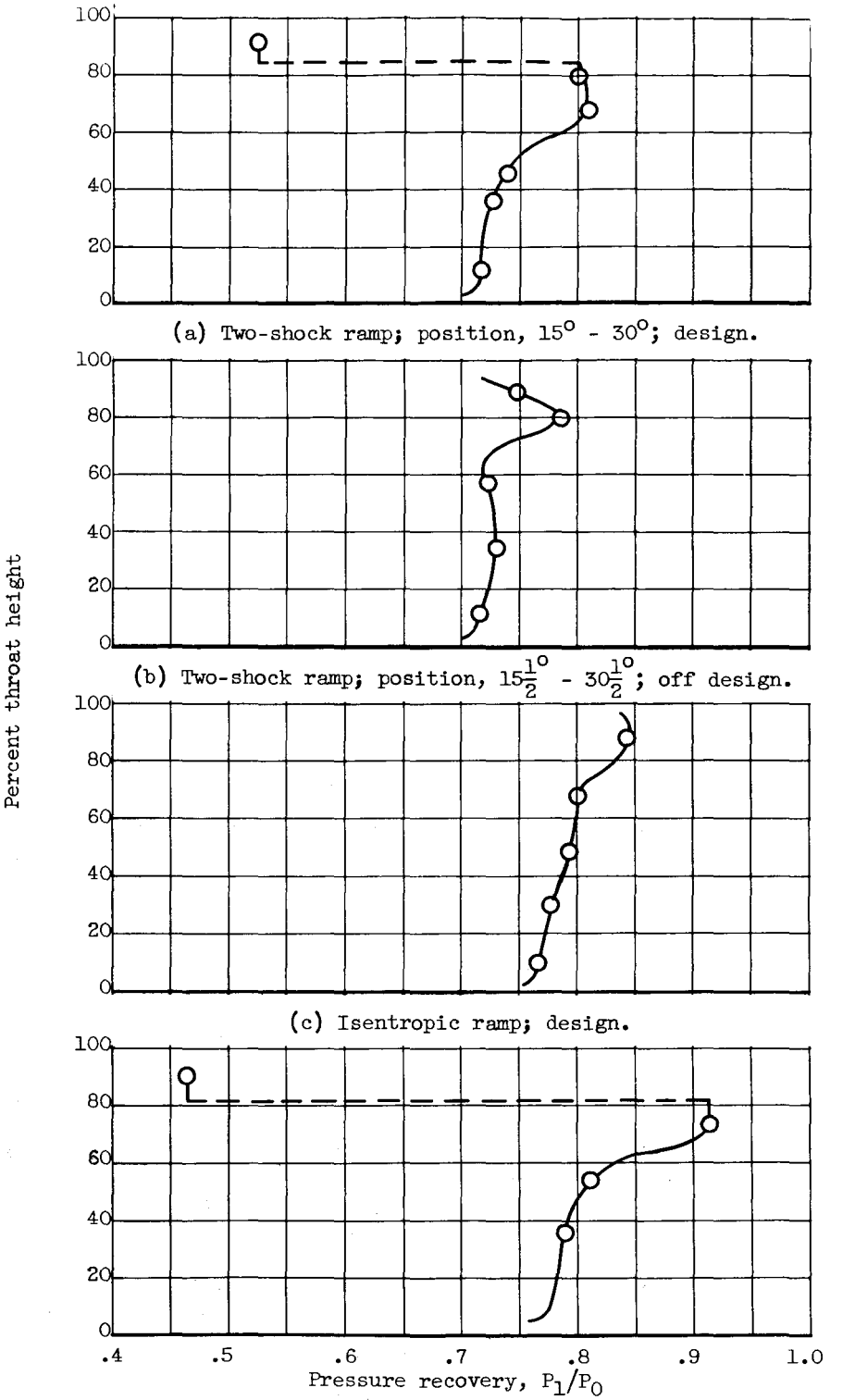

(a) Two-shock ramp; position, 15° - 30°; design.

(b) Two-shock ramp; position, $15\frac{1}{2}^{\circ}$ - $30\frac{1}{2}^{\circ}$; off design.

(c) Isentropic ramp; design.

(d) Isentropic ramp; off design.

Figure 8. - Total-pressure profiles at inlet throat.

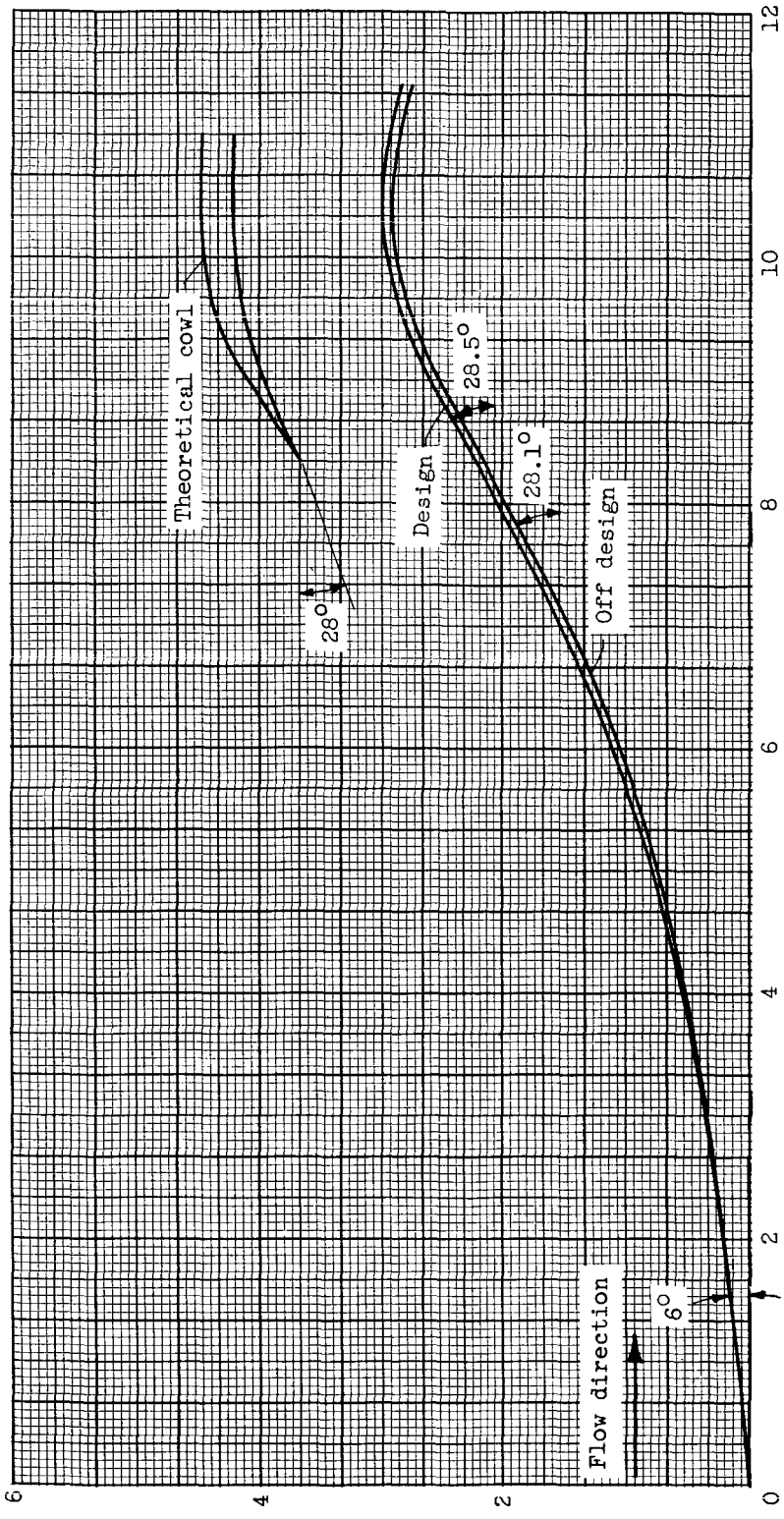

Figure 9. - Differences in isentropic-ramp contours at both design and off-design positions.

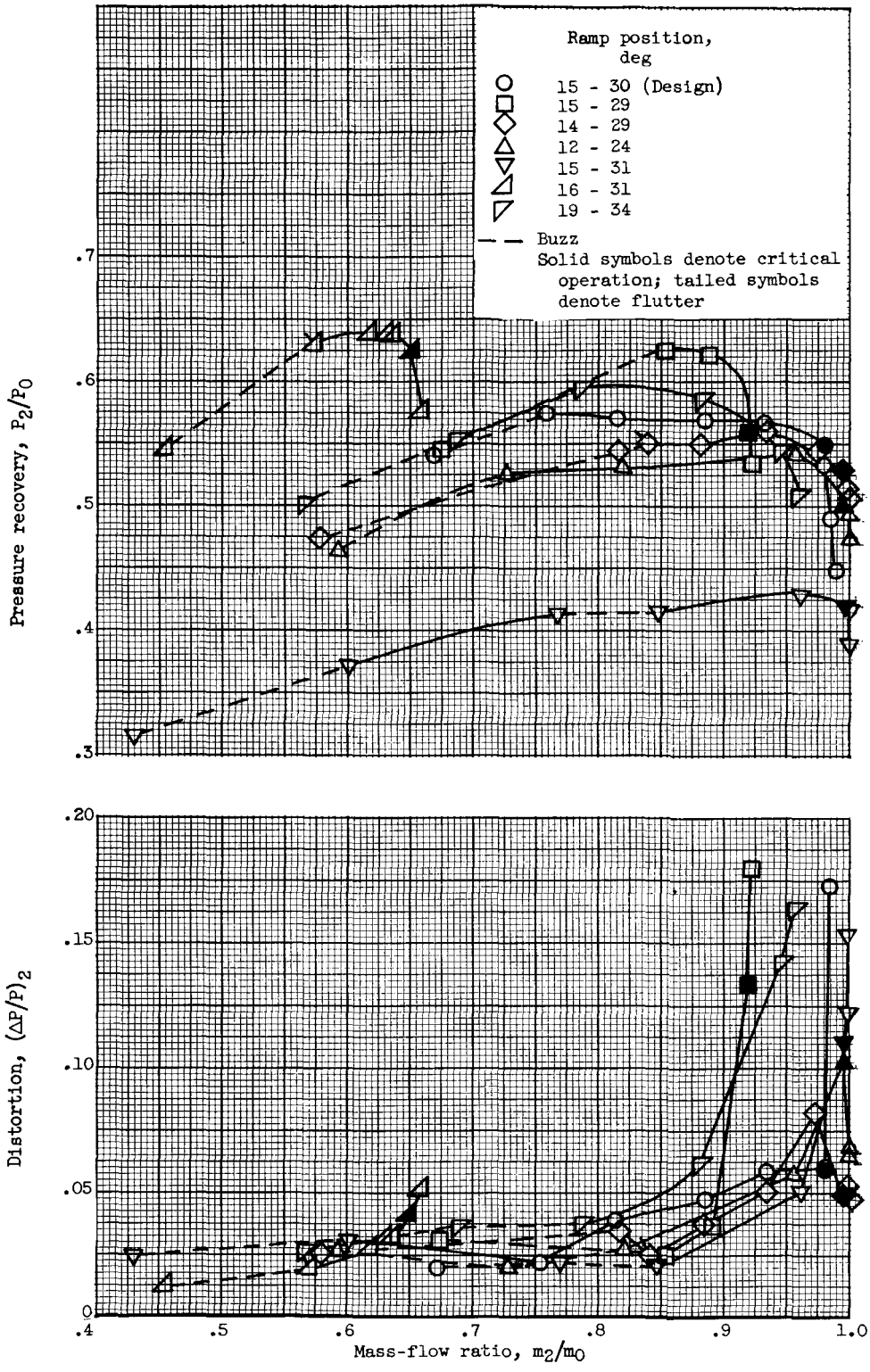

(a) Two-shock ramp; scoop-to-throat-height ratio, 0.

Figure 10. - Effect of off-design ramp position on basic diffuser performance.

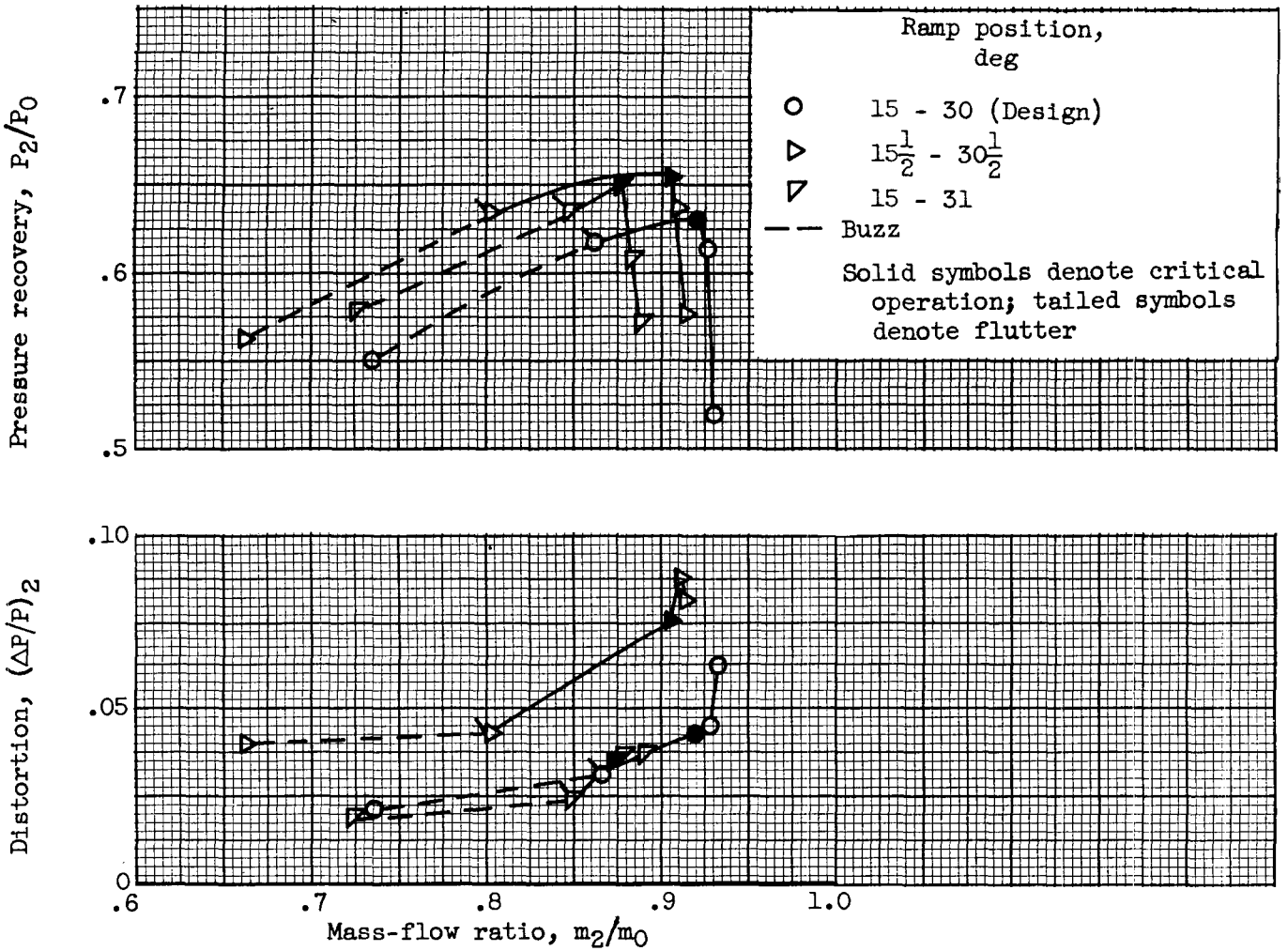

(b) Two-shock ramp; scoop-to-throat-height ratio, 0.112.

Figure 10. - Continued. Effect of off-design ramp position on basic diffuser performance.

CONFIDENTIAL

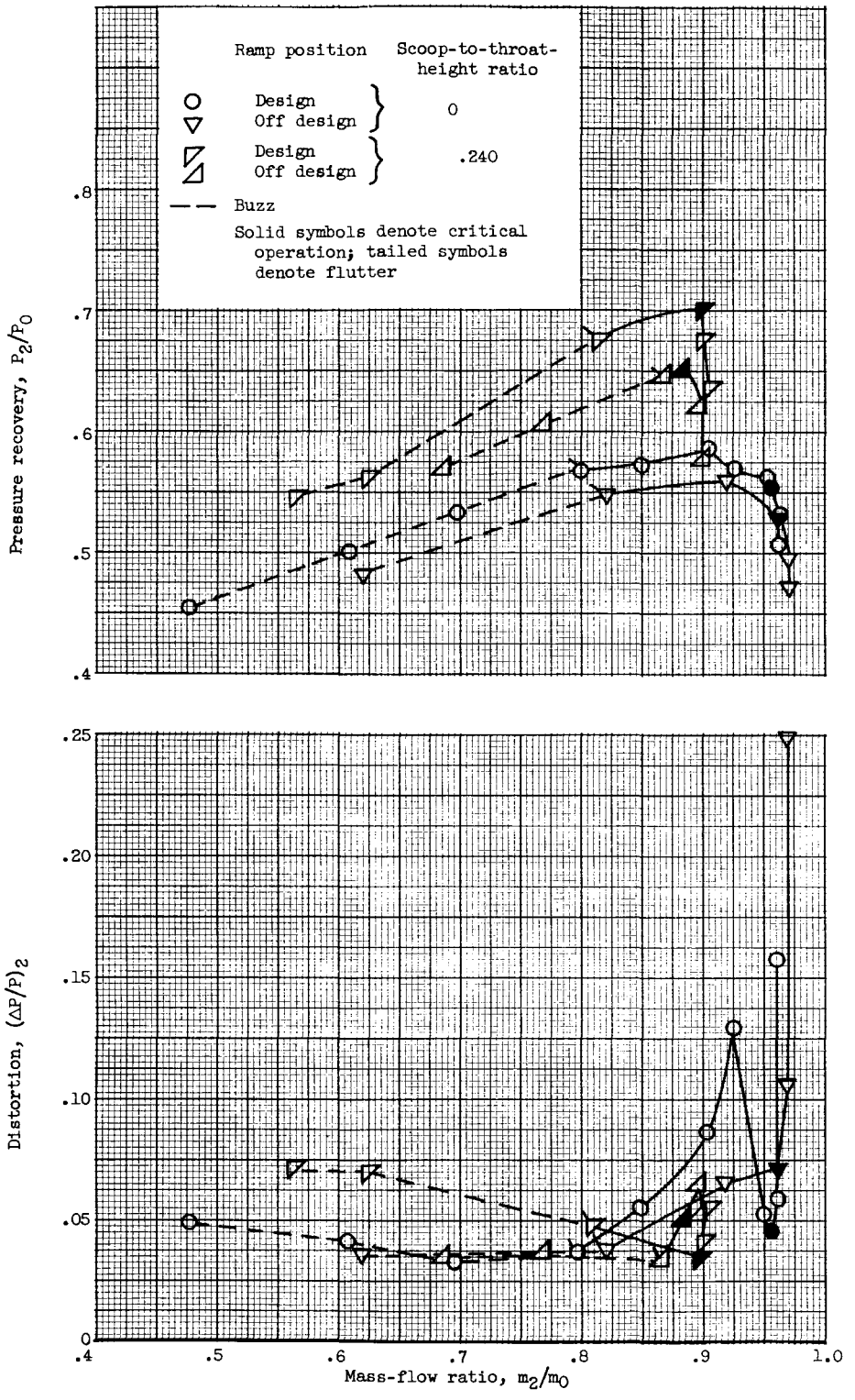

(c) Isentropic ramp.

Figure 10. - Concluded. Effect of off-design ramp position on basic diffuser performance.

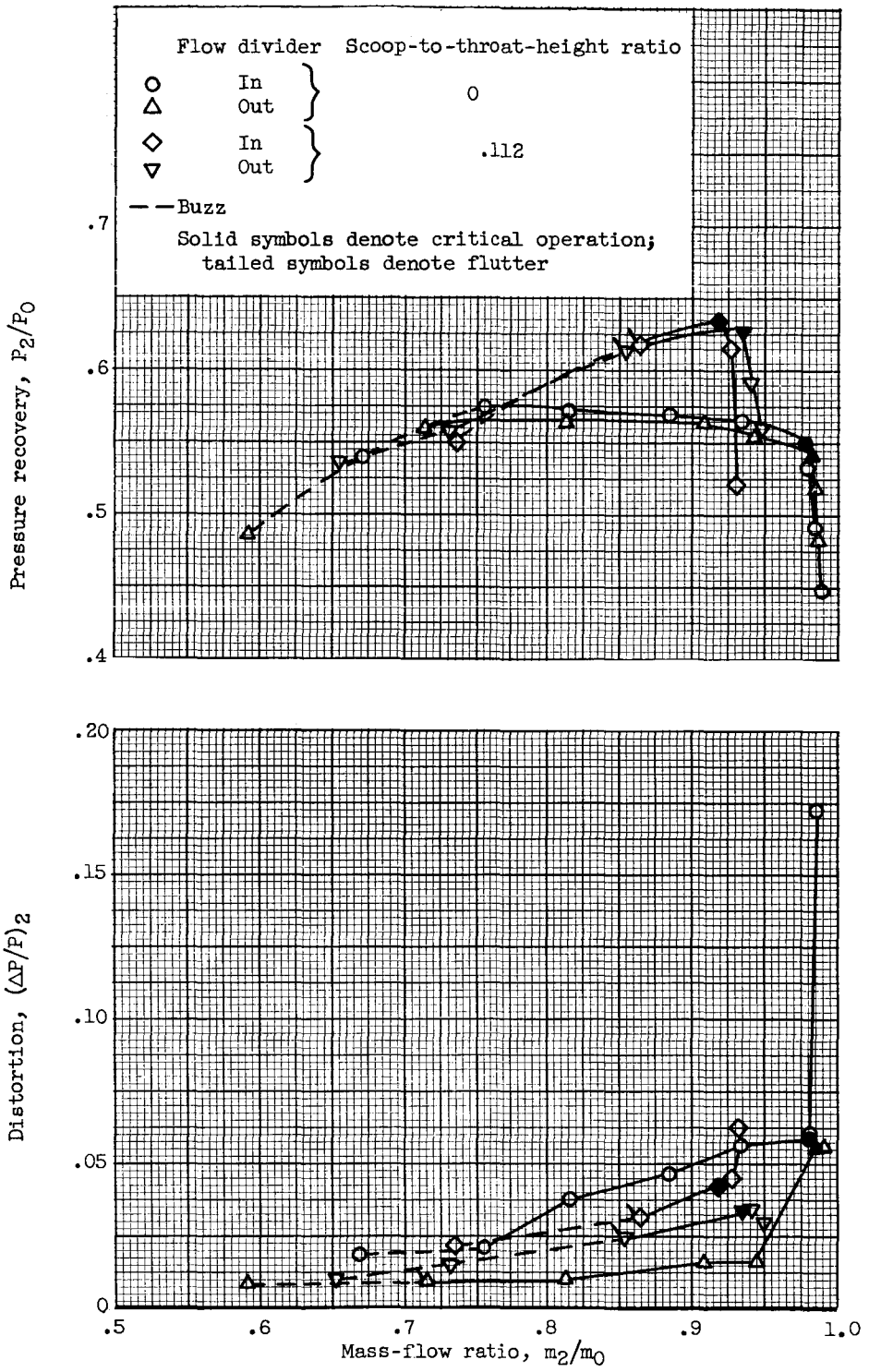

(a) Two-shock ramp.

Figure 11. - Effect on performance of removing flow divider of top bypass with design ramp positions.

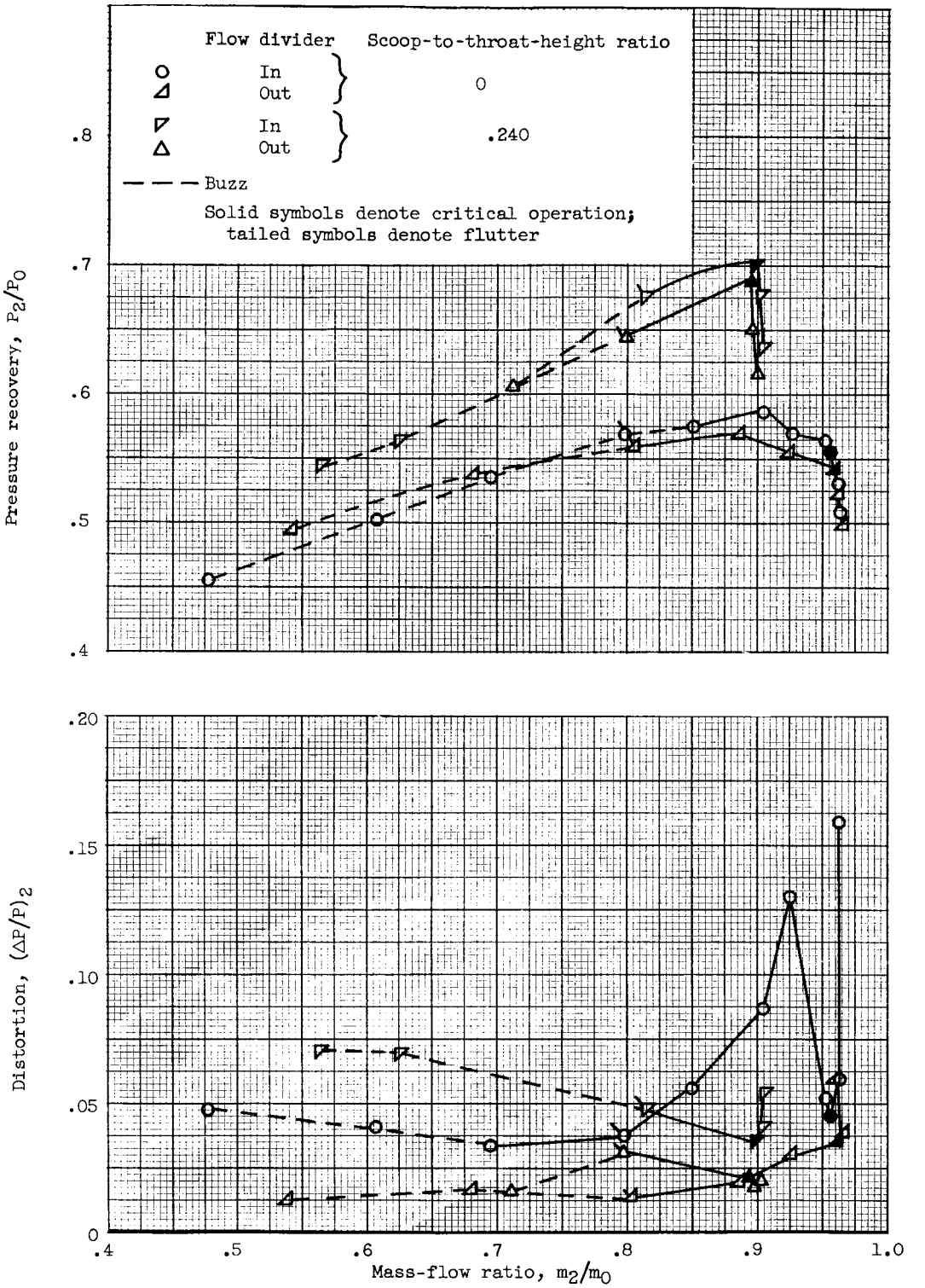

(b) Isentropic ramp.

Figure 11. - Concluded. Effect on performance of removing flow divider of top bypass with design ramp positions.

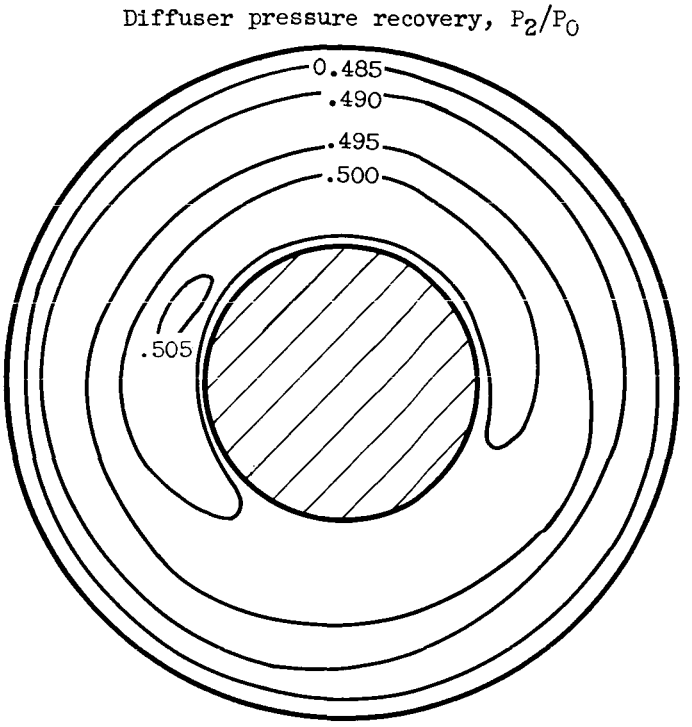

(a) Flow divider out; pressure recovery, 0.49; distortion, 0.04.

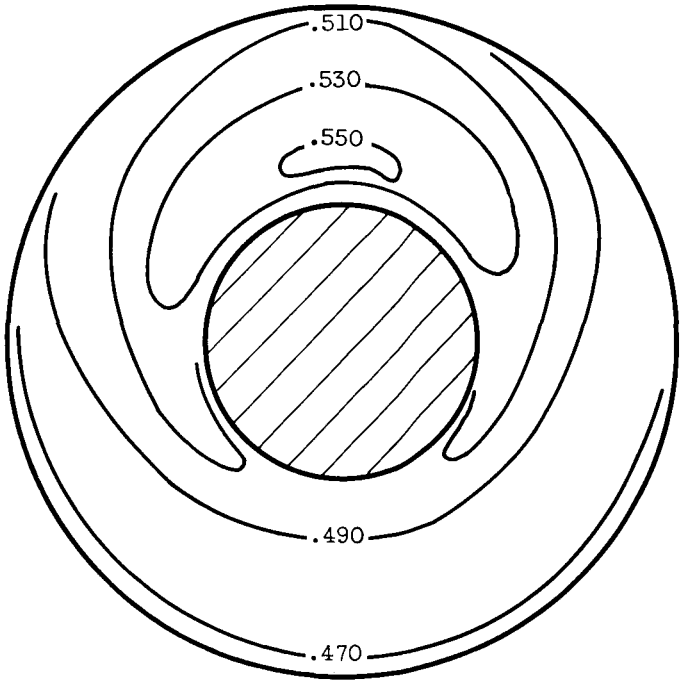

(b) Flow divider in; pressure recovery, 0.51; distortion, 0.16.

Figure 12. - Pressure-recovery contours at compressor face. Long diffuser plate; isentropic ramp at design position; scoop-to-throat-height ratio, 0; supercritical operation.

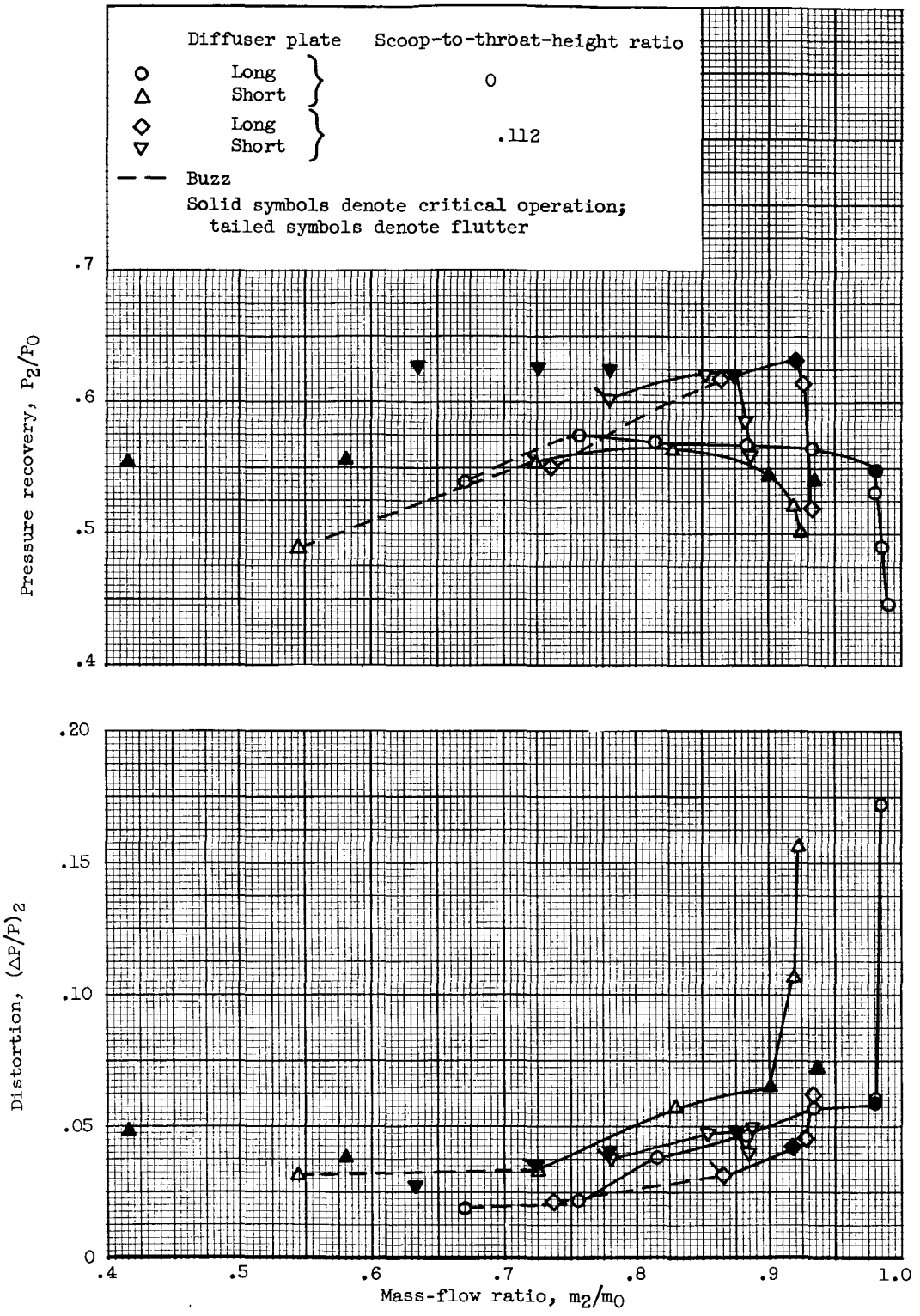

(a) Two-shock ramp.

Figure 13. - Effect on performance of bottom bypass with design ramp positions.

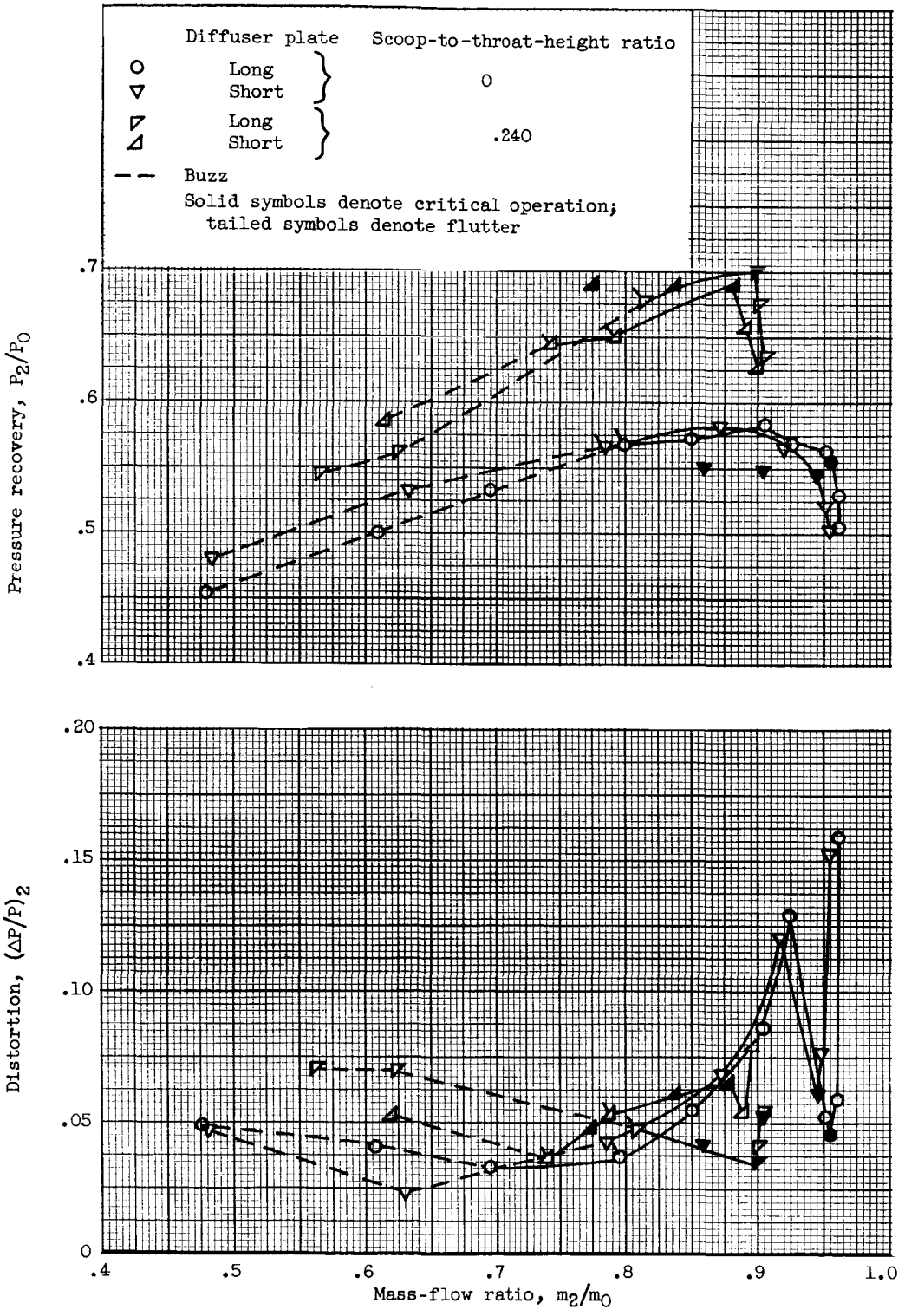

(b) Isentropic ramp.

Figure 13. - Concluded. Effect on performance of bottom bypass with design ramp positions.

NACA - Langley Field, Va.